ORIGINAL PAPER

Theoretical study of two-photon absorption properties and up-conversion efficiency of new symmetric organic π-conjugated molecules for photovoltaic devices

Zhong Hu · Vedbar S. Khadka · Wei Wang · David W. Galipeau · Xingzhong Yan

Abstract Organic material with high intensity of two-photon absorption (TPA) induced fluorescence can be used as the frequency up-converter materials for improving efficiency of the solar cells. In this work, the organic molecular structures were designed by symmetrically grafting two elongated conjugated linkers on a conjugated core and then adding donor groups at both terminals. Fluorene derivatives as a core acceptor, phenyl-ethynyl as the conjugated linker and diphenylamino or methyl-9H-carbozole as the donor end groups were selected. Quantum mechanical modeling techniques were applied to investigate the molecular electronic structure and properties. Absorption properties of these novel π-conjugated organic molecules were studied. The TPA cross-sections of these derivatives were calculated using few-states models, respectively. The effects of donor and acceptor groups on the TPA behaviors of these designed molecules were investigated. The up-conversion efficiency of designed molecules was also calculated.

Keywords Donor and acceptor · Frequency up-conversion · Organic conjugated materials · Quantum mechanics modeling · Two-photon absorption · Up-conversion efficiency

Z. Hu (✉) · D. W. Galipeau · X. Yan
Applied Photovoltaic Center, College of Engineering,
South Dakota State University,
Brookings, SD 57007, USA
e-mail: Zhong.Hu@sdstate.edu

V. S. Khadka
Department of Mathematics and Statistics, College of Engineering,
South Dakota State University,
Brookings, SD 57007, USA

W. Wang
Department of Mechanical Engineering, Binghamton University,
State University of New York,
Binghamton, NY 13902, USA

Introduction

Solar cells incorporate a p-n junction and their efficiency depends on the absorption properties of photoactive materials. For high efficiency, such materials should absorb photons in a broad range of the solar spectrum. Due to the Shockley-Queisser limit [1], sub-bandgap photons get lost and that, in turn, lowers the efficiency of the solar cells. To overcome this limit and to improve the efficiency of solar cells, up-converter based solar cell systems are being studied.

Two-photon absorption (TPA) induced emission is the frequency up-converter process which occurs due to the electronic excitation of a molecule induced by the simultaneous absorption of a pair of photons of the same energy. In 1931, Maria Goppert-Mayer [2] first explored the theoretical basis for two-photon quantum transitions (absorption and emission) in atoms. Though, her work was a major contribution in the field of nonlinear optics, it was not confirmed until the advent of the laser in the 1960s. In 1961, Kaiser, et al. made the first experimental observation of optical TPA processes [3]. Since then, many research works were stimulated to enter into the field of nonlinear optics [4–9].

Before the 1980s, the TPA was used as a spectroscopic tool to study the fundamental structural properties of different organic molecules. In the late 1980s, the real application of the TPA started to develop in various fields, such as three-dimensional optical data storage, photodynamic therapy, two-photon optical power limiting, two-photon three-dimensional micro-fabrication, two-photon excited laser scanning fluorescence microscopy, etc., in addition to the applications in photovoltaic cells for energy conversion [10–21].

Since organic molecules are less expensive to synthesize, flexible, lightweight, disposable and nontoxic; they can be customized at the molecular level to possess favorable properties. In recent years TPA properties have been studied

experimentally and theoretically for many organic molecules [21–40]. The research results showed that the value of TPA cross section (σ) determines the TPA properties and highly depends on the molecular structures. The conjugated length, structures of core, donor or acceptor of the molecules have great effects on its TPA properties. Organic molecules with various electron-donor (*D*) and electron-acceptor (*A*) attached symmetrically or asymmetrically to a conjugated bridge (π-center) are possible to have large σ values [30–36]. Varying *D* or *A* end groups, varying π conjugated center and varying effective conjugated length have been proved to be efficient ways for the design of molecules for finding large TPA cross section. However, the search for new compounds that possess the combined desirable properties, such as large TPA cross section with appropriate absorption spectrum (in the range of near-IR) for up-converter materials remains a big challenge.

In this work, several new organic molecules were designed by symmetrically grafting two elongated conjugated linker on a conjugated core and adding donor groups at both terminals. Fluorene derivatives show unique chemical and physical properties because they contain a rigid planar biphenyl unit, and the facile substitution at the remote C_9 position of fluorene can improve the solubility and processibility of luminescent materials without significant increase in steric interactions in the luminescent material backbone. Therefore, modified fluorene segments are used as a conjugated acceptor core [30, 37–40]. Phenylethynyl as the conjugated linker and diphenylamino or methyl-9H-carbozole as the effective electron-donor end groups were selected [41, 42]. Quantum mechanical modeling techniques were applied to investigate the molecular electronic structure and properties. The TPA cross-sections of these derivatives were calculated. The effects of donor end groups, conjugated acceptor cores, and conjugated linkers on the TPA behaviors of these designed molecules were investigated. Quantum mechanics modeling can be expected to develop new structure-property relations in these specific structures and provide insight for the design of up-converter materials.

Theory

TPA process

TPA is a nonlinear optical phenomenon. A simplified TPA process is shown in Fig. 1 [30]. TPA occurs in two ways [43–45]. The electron of molecule can be excited from ground state |0⟩ to excited state |*f*⟩ (final state) by the simultaneous absorption of two photons via a virtual level (as shown in Fig. 1a). The so-called virtual level is not real an intermediate level; its existence is allowed by quantum mechanics. The excited state can also be reached by stepwise TPA, which

includes two distinctive one-photon absorption (OPA) processes (as shown in Fig. 1b). The electron is firstly excited from ground state to a real intermediate state |*i*⟩ by the absorption of one photon with energy of $\hbar\omega_1$, and then it is excited from this intermediate state to final state by the absorption of another photon with energy of $\hbar\omega_2$. Such a nonlinear process is related to the second hyperpolarizability of molecule.

TPA cross section

The details of the electronic and structural description are refer to in [30]. The efficiency of TPA process can be characterized by the TPA cross section [30–32, 43–47]. The TPA cross section is related to the imaginary part of the third-order susceptibility (or the second hyperpolarizability),

$$\sigma = \frac{8\pi^2 h\omega^2}{n^2 c^2 N} \mathrm{Im}(\chi^{(3)}) = \frac{8\pi^2 h\omega^2}{n^2 c^2} \mathrm{Im}(\gamma) \tag{1}$$

where $\hbar$ is Plank constant divided by 2π; ω is the frequency of photon; *n* is the refractive index; *c* is the speed of light; and *N* is the number density of molecules. The TPA cross section can be obtained by evaluating the two-photon transition matrix elements, $S_{\alpha\beta}$, from the sum-over-state (SOS) expression [30, 47–51]. It is defined as [30, 31, 47, 52, 53]

$$S_{\alpha\beta} = \sum_i \left[\frac{\langle 0|\mu^\alpha|i\rangle\langle i|\mu^\beta|f\rangle}{\Delta E_i} + \frac{\langle 0|\mu^\beta|i\rangle\langle i|\mu^\alpha|f\rangle}{\Delta E_i} \right] \tag{2}$$

where $\Delta E_i = \hbar\omega_i - \hbar\omega_f/2$; μ^α and μ^β are the Cartesian components of the dipole moment operator μ, and $\alpha, \beta \in (x, y, z)$. The summation runs over all the intermediate states|*i*⟩, the ground state|0⟩, and the final state |*f*⟩.
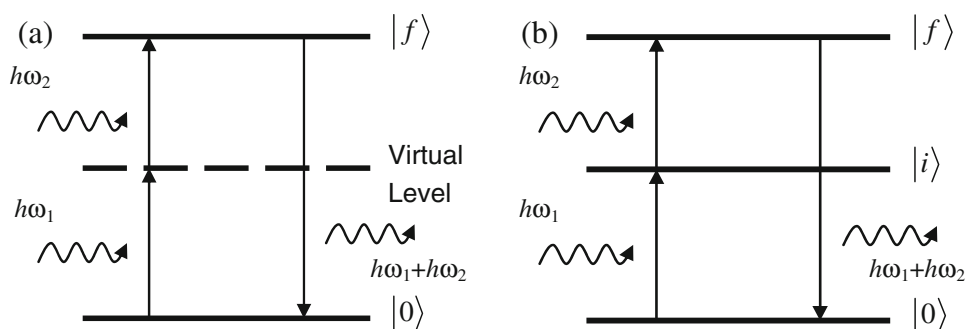
Using the two-photon transition matrix elements, $S_{\alpha\beta}$, which depend on transition dipole moments and excitation energies, the TPA transition probability, δ_{tp}, related on the polarization of the laser beams is given by [31]

$$\delta_{tp} = \sum_{\alpha\beta} \left[F \times S_{\alpha\alpha} S_{\beta\beta}^* + G \times S_{\alpha\beta} S_{\alpha\beta}^* + H \times S_{\alpha\beta} S_{\beta\alpha}^* \right] \tag{3}$$

where the coefficients *F*, *H*, and *G* are related to the polarization of the radiation sources and the summation goes over the molecular x, y and z axes. The values of *F*, *H*, and *G* are 2, 2, and 2 for a linearly polarized and -2, 3, and 3 for a circularly polarized monochromatic beam, respectively [31]. Eq. 3 is expanded to calculate the TPA cross section excited by a linearly polarized monochromatic beam as

$$\delta_{tp} = 6\left(S_{xx} + S_{yy} + S_{zz}\right)^2$$
$$+ 8\left(S_{xy}^2 + S_{yz}^2 + S_{zx}^2 - S_{xx}S_{yy} - S_{yy}S_{zz} - S_{zz}S_{xx}\right) \tag{4}$$

where S_{xx}, S_{yy}, S_{zz}, S_{xy}, S_{yz}, and S_{zx} are the two-photon transition elements obtained from Eq. 2.

Fig. 1 Two-photon absorption process

Few-states model for TPA cross section

However, the SOS method for calculating individual two-photon transition matrix elements uses many states which will often go beyond the computational capabilities of the hardware such as processor speed and memory. On the other hand, for some special molecular systems, such as molecules with symmetric structural configuration, the optical properties are found to be dominated by a few electronic states. In this case, the SOS expression only needs to include a few dominating states. The so-called few-states model [31, 47, 54–57] not only brings the SOS approach to a manageable extent, but also provides a better understanding for the revealed structure-to-property relations.

The three-states model

A simplified form of the SOS approach, was obtained from Eq. 2 when the excitation scheme is dominated by two major transitions, i.e., from the ground state $|0\rangle$ to the final excited state $|2\rangle$ via the intermediate state $|1\rangle$. The equation developed for calculating two-photon transition matrix elements $S_{\alpha\beta}$ using a three-states models can be expressed [56]

$$S_{\alpha\beta} = \left[\frac{\langle 0|\mu^{\alpha}|1\rangle\langle 1|\mu^{\beta}|2\rangle}{\Delta E} + \frac{\langle 0|\mu^{\beta}|1\rangle\langle 1|\mu^{\alpha}|2\rangle}{\Delta E}\right] \quad (5)$$

where $\Delta E = \hbar\omega_1 - \hbar\omega_2/2$, μ is the dipole moment operator, and $\alpha, \beta \in \{x, y, z\}$.

The four-states model

For molecules where the excitation scheme was not completely dominated by two transitions, the four-states model equation was developed for calculating two-photon transition matrix elements $S_{\alpha\beta}$ [56]

$$S_{\alpha\beta} = \left[\frac{\langle 0|\mu^{\alpha}|1\rangle\langle 1|\mu^{\beta}|3\rangle}{\Delta E_1} + \frac{\langle 0|\mu^{\beta}|1\rangle\langle 1|\mu^{\alpha}|3\rangle}{\Delta E_1}\right]$$
$$+ \left[\frac{\langle 0|\mu^{\alpha}|2\rangle\langle 2|\mu^{\beta}|3\rangle}{\Delta E_2} + \frac{\langle 0|\mu^{\beta}|2\rangle\langle 2|\mu^{\alpha}|3\rangle}{\Delta E_2}\right] \quad (6)$$

where $\Delta E_1 = \hbar\omega_1 - \hbar\omega_3/2$, and $\Delta E_2 = \hbar\omega_2 - \hbar\omega_3/2$. The four-states model was obtained from Eq. 2 which included two intermediate states $|1\rangle$ and $|2\rangle$ along with the ground state $|0\rangle$ and the final state $|3\rangle$.

TPA up-conversion efficiency

The TPA cross section is related to nonlinear absorption coefficient (β) which in turn determines the up-conversion efficiency (η). Up-conversion efficiency of an up-converter based on the TPA cross section (σ_{TPA}) is given by [58]

$$\eta = \frac{I_0 - I}{I_0} \times 100(\%) = \left[1 - e^{-\beta I_0 L}\right] \times 100(\%) \quad (7)$$

Where I is the output light intensity (GW/cm^2), L is the sample length (cm), β is the nonlinear absorption coefficient (cm/GW), and I_0 is the input light intensity (GW/cm^2). The nonlinear absorption coefficient (β) is calculated as

$$\beta = \frac{\sigma_{TPA} N_A C \times 10^3}{hc/\lambda} \times 10^{-56} \left(GW/cm^2\right) \quad (8)$$

Where σ_{TPA} is the TPA cross section in GM, N_A is Avogadro's Constant, C is concentration (mol/liter), h is Plank's Constant, c is speed of light (m/s), and λ is the wavelength of light (nm). The input light intensity is calculated as

$$I_0 = \frac{P_{in}}{(\pi\omega_0^2)\nu\tau_p} \times 10^5 \left(GW/cm^2\right) \quad (9)$$

Where ω_0 is radius of focus (μm), P_{in} is input power (mW), τ_p is pulse width (fs), and ν is pulse frequency (MHz).

Results and discussion

Molecule design

In order to design π-conjugated organic molecules with large TPA cross section, the first step was to find the π-conjugated framework of electron-withdrawing (acceptor) and/or electron-donating (donor) end groups, which possesses a highly polarizable electron cloud. The general

structural guideline of donor-π-donor usually referred to as push-push systems was a better structure for amplifying the TPA properties [59]. So, the donor–π-donor symmetric molecular structure was obtained by symmetrically grafting two elongated π-conjugated linker onto a π-conjugated acceptor (A) core and then adding donor (D) end groups. The conjugated linkers were used as linking group between acceptor and donor groups to assist intramolecular charge transfer between the electron-withdrawing and electron-donating groups, as shown in Fig. 2. Such molecules can be experimentally fabricated by means of Sonogashira or Heck coupling [59].

The second step was to find donor and acceptor groups having high electropositivty and electronegativity, respectively, and their combination in the molecular systems for getting high TPA cross section. Fluorene derivatives were selected as a core acceptor as they were successfully used in the design of multiphoton absorption [39, 40]. Phenylethynyl (PE) was selected as the conjugated linker to conduct the charge transfer from the end group to the core. For the donor (D) groups, diphenylamino, which is twisted shaped, and methyl-9H-carbazole, which is a planar shaped, compounds were selected [41, 42], see Fig. 3.

Molecules #1 to #4 were donor end group of methyl-9H-carbazole based and molecules #5 to #8 were donor end group of diphenylamino based, as shown in Fig. 4. These molecules show symmetry in structures and were grouped to compare their significance for TPA amplification. In each comparable group, the molecules have the same donor end group and linker (bridge), only change the acceptor cores.

Computational details

The software package Gaussian 03W is used to calculate molecular electronic structure and properties throughout this theoretical work [60], such as transition energy, wavelength, transition dipole moment and oscillator strength. These properties were then used to calculate the TPA cross-section. The geometric structure of each molecule was optimized at the Hartree-Fock level. Configuration Interaction Singlets (CIS) method was applied for investigating the important parameters of the excited states. These include excitation energies, transition dipole moments between the ground and excited states, transition dipole moments between different excited states, and the dipole moment difference between the ground and excited states. All calculations were carried out by using

Gaussian 03W quantum chemistry program, in which Hartree-Fock theory using a medium-sized basis set of 6-31G(d) (HF/6-31G(d)) was used for geometry optimization calculation. To make sure that all the optimized structures are minima for their potential energy, a vibrational frequency analysis was accomplished automatically by specifying both Opt and Freq within the route section for a submitted job. Furthermore, the configuration interaction with single excitations (CIS) method was used for obtaining other electro-optical data. The three-states and the four-states models (Eqs. 5 and 6) based on SOS formulas which involve the three and the four lowest excited states, respectively, were applied for calculating the TPA cross-section of each molecule.

HOMO, LUMO, and charge transfer

The simulated contour plots of the highest occupied molecular orbital (HOMO) and the lowest unoccupied molecular orbital (LUMO) of the designed molecules are shown in Fig. 5, which indicated the charge transfer directions. From Fig. 5 it can be clearly seen that molecules #2, #3, #4, #6, #7, and #8 have significant difference of molecular orbital distributions between HOMO and LUMO, especially molecule #8. The HOMO are distributed mainly on donor end-groups or donor to linker segments, and the LUMO are distributed mainly on the core acceptors, so that the charges are clearly transferring from the donors to the acceptors with the aid of the bridge (π-linker). On the other hand, molecules #1 and #5, which have no core acceptor, have much less difference of molecular orbital distributions between HOMO and LUMO and give no clear charge transferring directions.

TPA cross section parameters by the few-states model

Table 1 listed the calculated TPA cross section parameters of the designed molecules by using the three-states model, such as excitation energy (ΔE), the resultant transition dipole moments between the ground to the first excited states (μ_{01}) and the first excited to the second excited states (μ_{12}), the resonant two-photon transition matrix element ($S_{\alpha\beta}$), and the TPA cross section (σ_{TPA}). Each transition dipole moment between energy states had x-, y-, and z-axis components. So the two-photon transition matrix element S_{xy} was calculated by summing the product of x-axis transition dipole moment μ_{01} and y-axis transition dipole moment μ_{12},

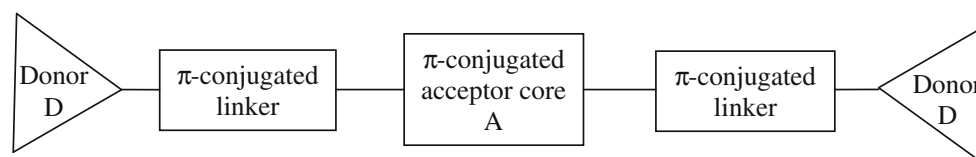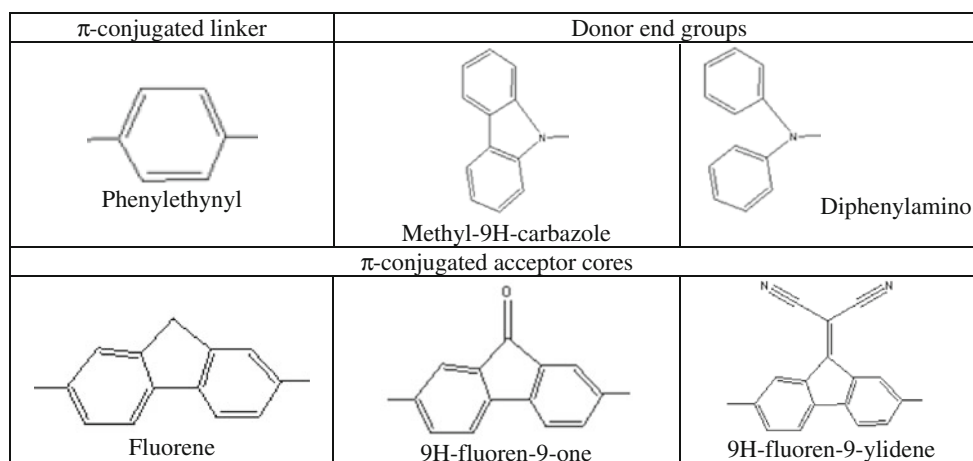**Fig. 2** Block diagram of organic up-converter molecular system

Fig. 3 Structures of π-conjugated linker, π-conjugated acceptor cores, and electron-donor end groups

π-conjugated linker	Donor end groups	
Phenylethynyl	Methyl-9H-carbazole	Diphenylamino
π-conjugated acceptor cores		
Fluorene	9H-fluoren-9-one	9H-fluoren-9-ylidene

and the product of y-axis transition dipole moment μ_{01} and x-axis transition dipole moment μ_{12}, and then dividing the sum with the excitation energy (ΔE) as described in Eq. 5. Based on the probability and orientation of different transition dipole moments, the two-photon transition matrix elements such as S_{xx}, S_{xy}, S_{xz}, S_{yx}, S_{yy}, S_{yz}, S_{zx}, S_{zy}, and S_{zz} were calculated and then used to calculate the TPA cross section (σ_{TPA}) using Eq. 4.

Table 2 listed the calculated TPA cross section parameters of the designed molecules by using the four-states model, such as excitation energies (ΔE_1 and ΔE_2), the resultant transition dipole moments between the ground to the first excited states (μ_{01}), the first excited to the third excited states (μ_{13}), the ground to the second excited states (μ_{02}), and the second excited to the third excited states (μ_{23}), the resonant two-photon transition matrix element ($S_{\alpha\beta}$), and the TPA cross section (σ_{TPA}), as described in Eq. 6. The four-states model differs from the three-states model as it has one more (two) intermediate states (the first and the second excited states) which
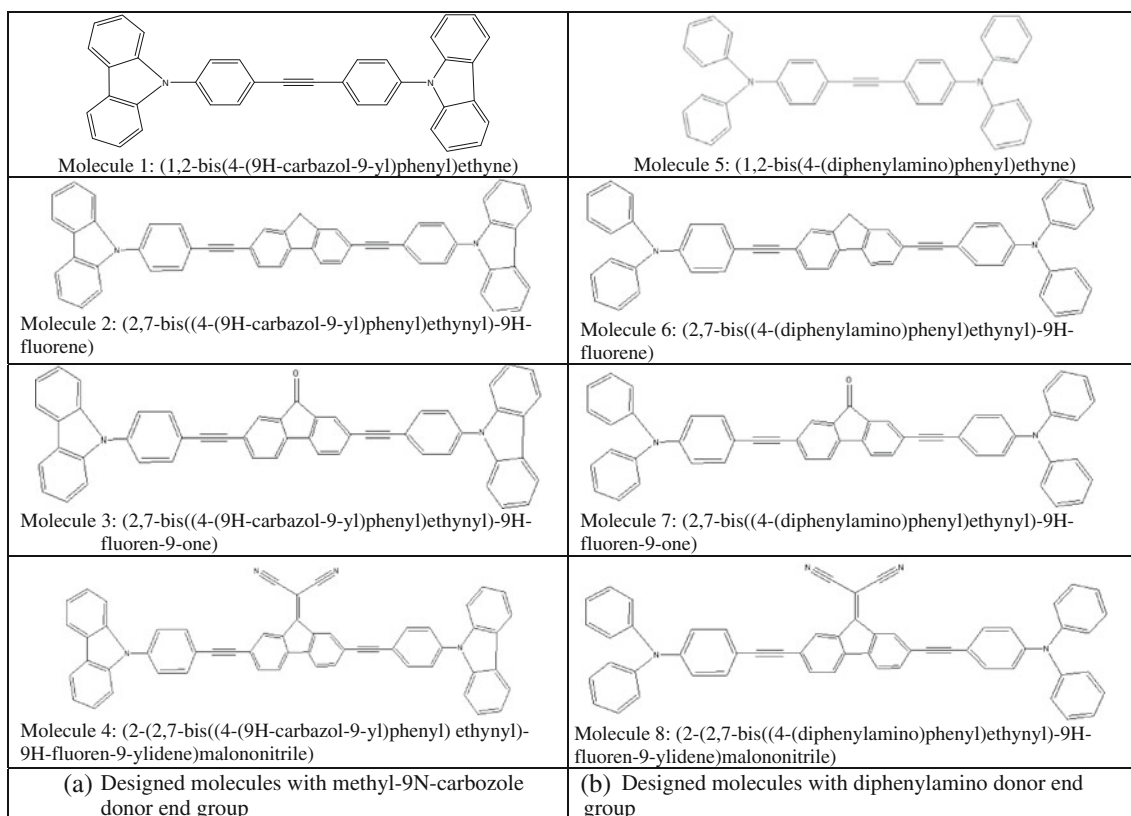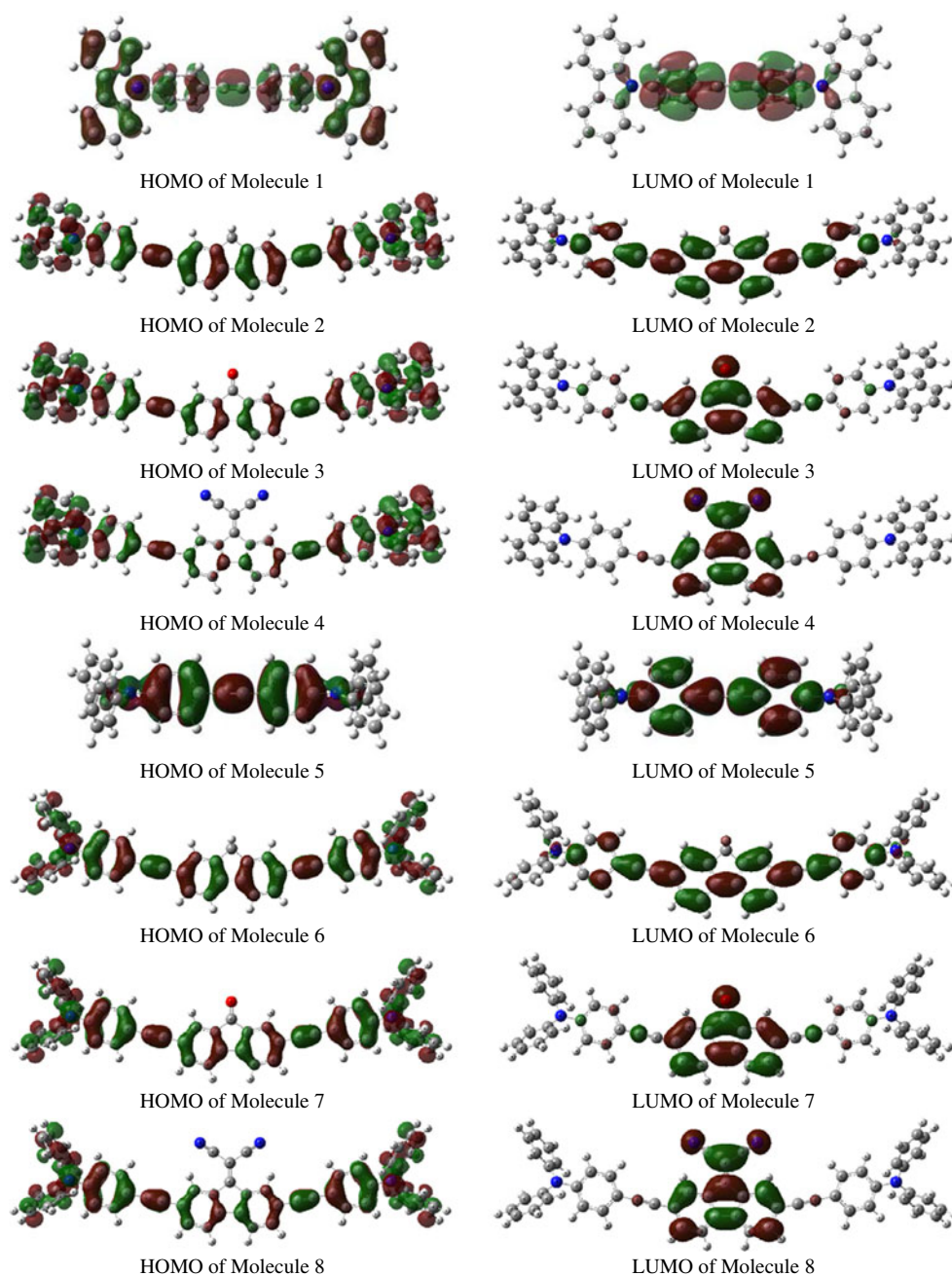

Molecule 1: (1,2-bis(4-(9H-carbazol-9-yl)phenyl)ethyne)

Molecule 2: (2,7-bis((4-(9H-carbazol-9-yl)phenyl)ethynyl)-9H-fluorene)

Molecule 3: (2,7-bis((4-(9H-carbazol-9-yl)phenyl)ethynyl)-9H-fluoren-9-one)

Molecule 4: (2-(2,7-bis((4-(9H-carbazol-9-yl)phenyl) ethynyl)-9H-fluoren-9-ylidene)malononitrile)

(a) Designed molecules with methyl-9N-carbozole donor end group

Molecule 5: (1,2-bis(4-(diphenylamino)phenyl)ethyne)

Molecule 6: (2,7-bis((4-(diphenylamino)phenyl)ethynyl)-9H-fluorene)

Molecule 7: (2,7-bis((4-(diphenylamino)phenyl)ethynyl)-9H-fluoren-9-one)

Molecule 8: (2-(2,7-bis((4-(diphenylamino)phenyl)ethynyl)-9H-fluoren-9-ylidene)malononitrile)

(b) Designed molecules with diphenylamino donor end group

Fig. 4 Eight newly designed symmetric organic π-conjugated molecules

Fig. 5 HOMO and LUMO of
the designed molecules

HOMO of Molecule 1   LUMO of Molecule 1

HOMO of Molecule 2   LUMO of Molecule 2

HOMO of Molecule 3   LUMO of Molecule 3

HOMO of Molecule 4   LUMO of Molecule 4

HOMO of Molecule 5   LUMO of Molecule 5

HOMO of Molecule 6   LUMO of Molecule 6

HOMO of Molecule 7   LUMO of Molecule 7

HOMO of Molecule 8   LUMO of Molecule 8

resulted in a ground to the third excited state transition. For molecules #1, #2, and #6, the three-states model gave the larger TPA cross sections than the four-states model did, indicating that the excitations of these molecules were dominated by two major transitions from the ground state to the second excited state via the first excited state. For molecules #3, #4, #5, #7, and #8, the three-states model gave smaller TPA cross sections than the four-states model did, indicating that the excitations of these molecules were not completely dominated by two transitions. So, the four-states model gave the larger TPA cross section for these molecules.

The data show that a large transition dipole moment yields a large two-photon transition matrix element, and in turn a large TPA cross section, such as molecules #8 and #6. On the other hand, a small transition dipole moment yields a small TPA cross section, such as molecules #1 and #5. Therefore, enhancement of the TPA cross section stemmed from the increased value of transition dipole moments between energy states.

It should be notice that CIS-computed transition energies are much larger than the corresponding experimental data and that of computed results obtained by the complete active space multiconfigurational second-order perturbation

Table 1 TPA cross section parameters of the designed molecules using the three-states model

Name	Excitation energy	Resultant transition dipole moment		Resonant TP transition matrix element	TPA cross-section
	ΔE (eV)	μ_{01} (D)	μ_{12} (D)	$S_{\alpha\beta}$ (AU)	σ_{TPA} (GM)
Molecule-1	2.29	9.28	0.19	$S_{XZ}=-3.39$	0.22
Molecule-2	1.73	14.29	0.94	$S_{XX}=65.67$	47.62
Molecule-3	1.38	5.65	0.037	$S_{XZ}=0.12$	0.002
Molecule-4	1.31	5.64	0.59	$S_{XX}=-21.57$	5.04
Molecule-5	2.04	9.24	0.055	$S_{XZ}=-0.929$	0.023
Molecule-6	1.90	14.11	2.06	$S_{XX}=-129.22$	193.47
Molecule-7	1.88	9.32	0.06	$S_{XZ}=-1.29$	0.01
Molecule-8	1.29	6.14	3.41	$S_{XY}=68.09$	62.82

(CASPT2) method. In some cases (particularly related to nucleic acid bases) some scaling factor (about 0.72) was suggested for CIS computed transition energies in order to compare with experimental data [61–66].

TPA cross section

The maximum TPA cross-section, the energy-gaps (the energy difference between HOMO and LUMO orbitals), the TPA wavelength, and the emission wavelength of the designed molecules are summarized in Table 3. These data were used to analyze the potential of these novel molecules as up-converter in photovoltaic devices based on their energy-gaps, emission spectra, and the TPA cross section. The maximum TPA cross section of each molecule corresponding to its TPA wavelength is shown in Fig. 6. The computed TPA wavelengths of the designed molecules, except molecule #3, are in the range of 480 to 690 nm, and they are falling into the visible part of the light spectra, which will be directly absorbed by most of the common photovoltaic cells. However, the TPA wavelength of molecule

#3 is in Near-IR range which cannot be absorbed by the solar cells, and its TPA cross section is relatively large, making it useful as the up-converter material.

Effects of acceptor cores and donor ends

It is noticed that adding acceptor cores will significantly improve the TPA cross sections, e.g., molecules #1 and #5 are formed without acceptor cores, and their maximum TPA cross section are 0.22 and 7.45 GM, respectively, which have the lowest values in each comparable group (group one of molecules #1 to #4 with methyl-9N-carbozole donor end group, and group two of molecules #5 to #8 with diphenylamino donor end group). Among the three acceptor cores of fluorene, 9H-fluoren-9-one, and 9H-fluoren-9-ylidene, the acceptor of 9H-fluoren-9-ylidene results in a very large TPA cross section when it is incorporated with diphenylamino donor end group, e.g., molecule #8 having TPA cross section of 493.52 GM (the largest value among all the eight designed molecules). The acceptor of fluorene may also result in a large TPA cross section when it is

Table 2 TPA cross section parameters of the designed molecules using the four-states model

Name	Excitation energy		Resultant transition dipole moment				Resonant TP transition matrix	TPA cross-section
	E_1(eV)	E_2(eV)	μ_{01} (D)	μ_{13} (D)	μ_{02}(D)	μ_{23} (D)	Element $S_{\alpha\beta}$ (AU)	σ_{TPA}(GM)
Moleulce-1	2.29	2.79	9.28	0.24	2.12	1.33	$S_{XX}=0.1746$	4×10^{-4}
Molecule-2	1.46	2.17	14.29	0.007	2.26	0.044	$S_{XZ}=-8.739$	0.004
Molecule-3	0.78	1.09	5.65	2.48	5.0×10^{-4}	9.3×10^{-3}	$S_{XY}=75.45$	73.74
Molecule-4	1.31	2.42	5.64	3.36	5.19	0.86	$S_{XY}=-68.69$	68.37
Molecule-5	2.04	3.04	9.24	0.98	0.27	0.22	$S_{XZ}=-16.53$	7.45
Molecule-6	1.61	2.21	14.11	0.28	2.23	2.05	$S_{XY}=19.33$	7.19
Molecule-7	1.57	1.83	9.32	2.19	2.5×10^{-4}	0.03	$S_{XY}=54.84$	44.5
Molecule-8	1.25	2.30	6.14	4.27	13.3	0.86	$S_{XX}=-216.0$	493.52

Table 3 Summary of maximum TPA cross-section, energy gap between HOMO and LUMO, TPA wavelength, and emission wavelength of the designed molecules

Name	Max TPA cross-section (GM)	Energy gap (eV)	TPA wavelength (nm)	Emission wavelength (nm)
Molecule-1	0.22	5.0918	487.0 (Blue Band)	348
Molecule-2	47.63	4.1859	592.4 (Orange Band)	423
Molecule-3	73.74	3.0837	804.1 (Near IR Band)	575
Molecule-4	68.37	3.7434	662.4 (Red Band)	473
Molecule-5	7.45	5.0973	486.5 (Blue Band)	347
Molecule-6	193.47	4.4126	562.0 (Green Band)	401
Molecule-7	44.50	4.0270	615.8 (Orange Band)	440
Molecule-8	493.52	3.6473	679.9 (Red Band)	486

incorporated with diphenylamino donor end group, e.g., molecule #6 having TPA cross section of 193.47 GM (the second largest value among the eight molecules). However, the three acceptors may result in relatively large values of TPA cross sections without significant difference when they are incorporated with Methyl-9H-carbazole donor end groups, e.g., molecules #2, #3, and #4 having TPA cross sections of 47.63 GM, 73.74 GM, and 68.37 GM, respectively.

Up-conversion efficiency

Table 4 lists the up-conversion efficiency data of the designed molecules under 700 mW of input power and 1 mole per liter concentration calculated using Eqs. 7, 8 and 9, assuming using a Ti:sapphire femtosecond laser beam focused on a sample to induce fluorescence [29]. In the calculation, the pulse frequency ν is 86 MHz, the radius of focus is 8.089 μm, and the pulse

width is 57 fs. The data shows that larger TPA cross section yields higher up-conversion efficiency when all other parameters are constant.

Among these eight novel molecules, molecule #3 would be a good candidate as it has the smallest energy-gap of 3.0837 eV and large TPA cross section of 73.74 GM. Furthermore, as an up-converter, it can absorb two photons of 1.54 eV (804.1 nm) simultaneously and emit a photon of 2.16 eV (575 nm). So, it appears to be suitable as an up-converter in aluminum arsenide and copper gallium selenide solar cells which have an energy-gap of 1.7 eV (730 nm). Such solar cells cannot absorb photons smaller than 1.7 eV (wavelength greater than 730 nm). Therefore, when useing molecule #3 as an up-converter, it can absorb photons from 1.7 eV to 1.54 eV (730 nm to 804 nm) and up-convert them to a higher energy level above the energy-gap (1.7 eV). These higher energy photons will be reemitted back to the solar cells to be absorbed by the solar cells.
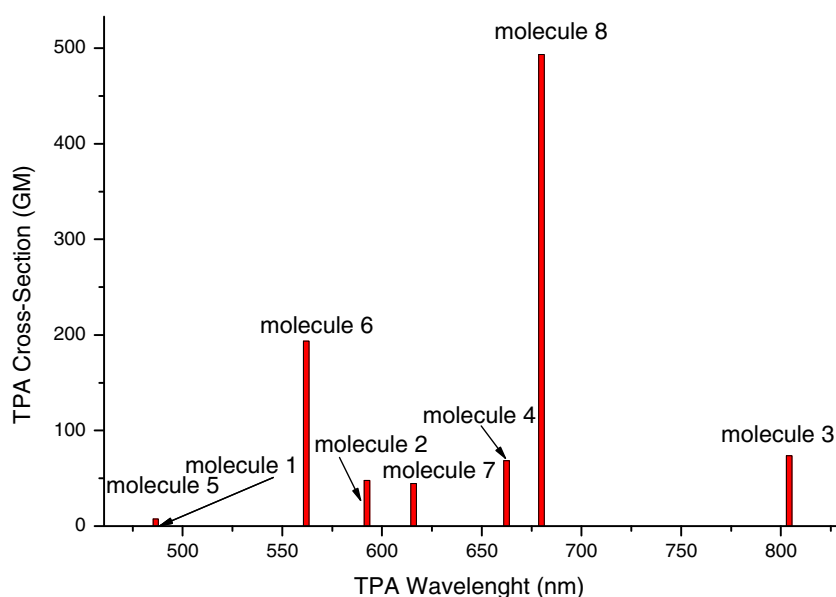

Fig. 6 Maximum TPA cross-sections of designed molecules

Table 4 Efficiency of the designed molecules as up-converter materials in photovoltaics

Name	Input power (mW)	TPA cross-section (GM)	Concentration C (mol/liter)	I_o (GW/cm^2)	β (cm/GW)	Efficiency (η) %
Molecule -1	700	0.221	1	6.9440E+01	2.6770E-06	0.018
Molecule -2	700	47.62	1	6.9440E+01	5.7682 E-04	3.926
Molecule -3	700	73.74	1	6.9440E+01	8.9321E-04	6.014
Molecule -4	700	68.37	1	6.9440E+01	8.2817 E-04	5.588
Molecule-5	700	7.45	1	6.9440E+01	9.0242 E-05	0.624
Molecule -6	700	193.47	1	6.9440E+01	2.3378 E-03	15.018
Molecule -7	700	44.5	1	6.9440E+01	5.3903 E-04	3.6738
Molecule -8	700	493.52	1	6.9440E+01	5.9780 E-03	33.973

ASTM G197-03 reference extraterrestrial solar spectrum was used to predict the solar efficiency of 1.1 eV energy-gap solar cells and found it to be 44% as predicted by Shockley et al. [1]. Using the same method, the predicted efficiencies of aluminum gallium arsenide and copper gallium selenide solar cells were found to be 35.95%. When molecule #3 was used as an up-converter in such solar cells, efficiencies was found to be 43.22%. So, the maximum up-conversion efficiency by molecule #3 was 7.26%. Based on the TPA cross section, the up-conversion efficiency of molecule #3 under 700 mW input power and 1 mole per liter concentration was found to be 6.014% as listed in Table 4. Therefore, using TPA cross section and band width of up-converted frequency of molecule #3, the possible up-conversion efficiency achieved was 0.436% ($\approx$6.014% of 7.26). Of course, the TPA cross section of this molecule could be further improved so that makes it feasible in the application with higher efficiency.

Molecule #8 would be another good candidate since it has a very large TPA cross section of 493.52 GM and a relative smaller energy-gap than all the molecules except molecule #3. If the TPA wavelength could be expended longer that would be closer to the application purpose.

Conclusions

Novel π-conjugated organic molecules to promote charge transfer and enhance TPA were designed based on the general structural guideline of donor-π linker-acceptor- π linker-donor symmetry. Fluorene derivatives as a core acceptor, phenylethynyl as the conjugated linker and diphenylamino or methyl-9H-carbozole as the donor end groups were selected. Quantum mechanical modeling techniques were applied to investigate the molecular electronic structure and properties. The following conclusions have been reached.

Donor-acceptor combination on organic π-conjugated molecules can improve charge transfer and increase the transition dipole moments between energy states and in turn contribute to the enhancement of TPA cross section in a π-conjugated molecular system.

The electronic and optical data from modeling can be used to calculate the TPA cross section.

Molecules without the acceptor cores have negligible TPA cross sections and therefore need to have both donor and acceptor groups to be good two-photon absorbers.

Molecules with 9H-fluoren-9-one as the acceptor core, phenylethynyl as conjugated linker, and methyl-9H-carbazole as the donor end group can be suitable as up-converters in aluminum gallium arsenide and copper gallium selenide solar cells because of the small energy-gap.

Molecules with fluorene as an acceptor core, phenylethynyl as conjugated linker, and diphenylamino or methyl-9H-carbazole as the donor end group can be suitable as up-converters in high energy-gap solar cells like silicon carbide.

Molecule with 9H-fluoren-9-ylidene as an acceptor core, phenylethynyl as conjugated linker, and diphenylamino as the donor end group can achieve very large TPA cross section, if the structure could be further optimized to lower the energy-gap, it would be a good candidate as an up-converter in aluminum gallium arsenide and copper gallium selenide solar cells.

The TPA process can be feasible if the power of the incident light is high enough, so that up-conversion efficiency will be high enough to improve the total efficiency of the solar cells.

References

1. Shockley W, Queisser HJ (1961) Detailed balance limit of efficiency of p-n junction solar cells. J Appl Phys 32:510–519

2. Goppert-Mayer M (1931) Two-quantum processes. Ann Phys (Leipzig) 9:273–294

3. Kaiser W, Garrett CG (1961) Two-photon excitation in CaF2:Eu2+. Phys Rev Lett 7:229–231

4. Zubov BV, Kulevskii LA, Makarov VP, Murina TM, Prokhorov AM (1969) Two-photon absorption in germanium. JETP Lett 9:165–167

5. Jaiswal AK, Agarwal GS (1969) Photoelectric detection with two-photon absorption. J Opt Soc Amer 59:1446–1452

6. Yee JH (1969) Theoretical calculation of photoconductivity induced by a multiple-photon absorption process in semiconductors. Appl Phys Lett 15:431–433

7. Frohlich D, Staginnus B, Onodera Y (1970) Two-photon spectroscopy in CsI and CsBr. Phys Status Solidi (B) 40:547–556

8. Srivastava GP, Goyal ML, Shyam R, Gupta SC (1972) Two-photon excitation in phenanthrene. J Opt Soc Am 62:827

9. Aslanidi EB, Tikhonov EA, Shpak MT (1972) Two-photon absorption of impurity molecules enhanced by matrix. Opt Commun 6:163–165

10. Parthenopoulos DA, Rentzepis PM (1989) Three-dimensional optical storage memory. Science 245:843–845

11. Dvornikov AS, Rentzepis PM (1995) Accessing 3D memory information by means of nonlinear absorption. Opt Commun 119:341–346

12. Kawata S (1998) Application of two-photon absorption to three-dimensional micro-fabrication and high density data storage. J Optoelectron Laser 9:290–292

13. Denk W, Strickler JH, Webb WW (1990) *Two*-photon laser scanning fluorescence microscopy. Science 248:73–76

14. Denk W, Svoboda K (1997) Photon upmanship: why multiphoton imaging is more than a gimmick. Neuron 18:351–357

15. Sakadzic S, Demirbas U, Mempel TR, Moore A, Ruvinskaya S, Boas DA, Sennaroglu A, Kaertner FX, Fujimoto JG (2008) Multiphoton microscopy with a low-cost and highly efficient Cr:LiCAF laser. Opt Express 16:20848–20863

16. Helmchen F, Denk W (2005) Deep tissue two-photon microscopy. Nat Methods 2:932–940

17. Wachter EA, Partridge WP, Fisher WG, Dees HC, Petersen MG (1998) Simultaneous two-photon activation of type-I photodynamic therapy agents. Proc SPIE 3269:68–75

18. Tutt LW, Boggess TF (1993) A review of optical limiting mechanisms and devices using organics, fullerenes, semiconductors and other materials. Prog Quantum Electron 17:299–3

19. Spangler CW, Elandaloussi EH, Casstevens MK, Kumar DN, Weibel JF, Burzynski R (1999) Design and synthesis of new optical-power-limiting chromophores with enhanced two-photon absorption. Proc SPIE 3798:117

20. Maruo S, Nakamura O, Kawata S (1997) Three-dimensional microfabrication with two-photon-absorbed photopolymerization. Opt Lett 22:132–134

21. Ray PC, Sainudeen Z (2006) Very large infrared two photon absorption cross section of asymmetric zinc porphyrin aggregates: role of intermolecular interaction and donor-acceptor strengths. J Phys Chem A 110:12342–11347

22. Zhou X, Ren AM, Feng JK, Liu XJ (2003) Theoretical study of two-photon absorption properties of a series of double-layer paracyclophane derivatives. J Phys Chem A 107:1850–1858

23. Zhou X, Ren AM, Feng JK, Liu XJ (2004) Theoretical studies on the one- and two- photon absorption of tetrabenzoporphyrins and phthalocyanines. Can J Chem 82:19–26

24. Boni LD, Constantino CJL, Misoguti L, Aroca RF, Zilio SC, Mendonca CR (2003) Two-photon absorption in perylene derivatives. Chem Phys Lett 371:744–749

25. Lin N, Zhao X, Yang JX, Jiang MH, Liu JC, Wang CK, Shi W, Meng J, Weng J (2006) Theoretical study of one-, two-, and three-photon absorption properties for a series of Y-shaped molecules. J Chem Phys 124:024704

26. Zhao Y, Xiao L, Wu F, Fang X (2007) Two-photon absorption properties of malononitrile derivatives. Opt Mater 29:1206–1210

27. Qian Y, Zhu XQ, Huang W, Lu CG, Lin GQ, Cui YP (2008) Two-photon absorption and upconversion fluorescence by using a femtosecond Ti:sapphire laser in symmetrical chromophores. J Funct Mater 39:1774–1777

28. Ray D, Nag A, Goswami D, Bharadwaj PK (2009) Acyclic donor-acceptor-donor chromophores for large enhancement of two-photon absorption cross-section in the presence of Mg(II), Ca(II) or Zn(II) ions. J Lumin 129:256–262

29. Yan XY, Goodson T, Imaoka T, Yamamoto K (2005) Up-converted emission in a series of phenylazomethine dendrimers with a porphyrin core. J Phys Chem 109:9321–9329

30. Hu Z, Wang W, Khadka VS, Galipeau DW, Yan XZ (2011) Quantum mechanical modelling and calculation of two-photon absorption properties of new class 'Λ'-shaped conjugated molecules. Mol Simul 37:431–439

31. Wang CK, Macak P, Luo Y, Agren H (201) Effects of π centers and symmetry on two-photon absorption cross sections of organic chromophores. J Chem Phys 114:9813-9820

32. Albota MA, Beljonne D, Brédas JL, Ehrlich JE, Fu JY, Heikal AA, Hess SE, Kogej T, Levin MD, Marder SR, McCord-Maughon D, Perry JW, Röckel H, Rumi M, SubramaniamG WWW, Wu XL, Xu C (1998) Design of organic molecules with large two-photon absorption cross sections. Science 281:1653–1656

33. Kim OK, Lee KS, Woo HY, Kim KS, He GS, Swiatkiewicz J, Prasad PN (2000) New class of two-photon-absorbing chromophores based on dithienothiophene. Chem Mater 12:284–286

34. Reinhardt BA, Brott LL, Clarson SJ, Dillard AG, Bhatt JC, Kannan R, Yuan L, He GS, Prasad PN (1998) Highly active two-photon dyes: design, synthesis, and characterization toward application. Chem Mater 10:1863–1874

35. Ohta K, Kamada K (2006) Theoretical investigation of two-photon absorption allowed excited states in symmetrically substituted diacetylenes by *ab initio* molecular-orbital method. J Chem Phys 124:124303

36. Kim DY, Ahn TK, Kwon JH, Kim D, Ikeue T, Aratani N, Osuka A, Shigeiwa M, Maeda S (2005) Large two-photon absorption (TPA) cross-section of directly linked fused diporphyrins. J Phys Chem A 109:2996–2999

37. Klaerner G, Miller RD (1998) Polyfluorine derivatives: effective conjugation lengths from well-defined oligomers. Macromolecules 31:2007–2009

38. Feng L, Chen Z (2005) Synthesis, characterization and photophysical processes of fluorene derivative containing naphthalene nucleus. Spectrochim Acta A Mol Biomol Spectrosc 61:2505–2509

39. Belfield KD, Bondar MV, Hales JM, Morales AR, Przhonska OV, Schafer KJ (2005) One- and two-photon fluorescence anisotropy of fluorene derivatives. J Fluoresc 15:3–11

40. Cumpston B, Lipson M, Marder SR, Perry JW (2007) Two-photon or higher-order absorbing optical materials for generation of reactive species. United States Patent, Patent No. US 7,235,194 B2, Date of Patent: Jun. 26, 2007

41. Leung MK, Chou MY, Su YO, Chiang CL, Chen HL, Yang CF, Yang CC, Lin CC, Chen HT (2003) Diphenylamino group as an effective handle to conjugated donor–acceptor polymers through electropolymerization. Org Lett 5:839–842

42. Yang CH, Liao SH, Sun YK, Chuang YY, Wang TL, Shieh YT, Lin WC (2010) Optimization of multiple electron donor and acceptor in carbazole-triphenylamine-based molecules for application of dye-sensitized solar cells. J Phys Chem C 114:21786–21794

43. Kuzyk MG, Dirk CW (1998) Characterization techniques and tabulations for organic nonlinear optical materials. Dekker, , New York

44. Karotki A (2003) Simultaneous two-photon absorption of tetrapyrrrolic molecules: from femtosecond coherence experiments to photodynamic therapy. Ph.D. Thesis, Department of Physics, Montana State Universiy, Bozaman

45. Levenson MD, Kano SS (1988) Introduction to nonlinear laser spectroscopy. Academic, New York

46. Laud BB (1991) Lasers and non-linear optics. Wiley, New Delhi

47. Zhao K (2007) Theoretical study of light-molecule nonlinear interactions, Ph.D. Thesis, Department of Theoretical Chemistry, Royal Institute of Technology, Stockhlm

48. Liu XJ, Feng JK, Ren AM, Cheng H, Zhou X (2004) Calculations on the octupolar molecules with enhanced two-photon absorption cross sections based on the Zn(II) and Cu(I) as centers. J Chem Phys 120:11493–11499

49. Beljonne D, Brédas JL, Cha M, Torruellas WE, Stegeman GI, Hofstraat JW, Horsthuis WHG, Möhlmann GR (1995) Two-photon absorption and third-harmonic generation of di-alkylamino-nitro-stilbene (DANS): a joint experimental and theoretical study. J Chem Phys 103:7834–7843

50. Willetts A, Rice JE, Burland DM, Shelton DP (1992) Problems in the comparison of theoretical and experimental hyperpolarizabilities. J Chem Phys 97:7590–7599

51. Liu XJ, Feng JK, Ren AM, Cheng H, Zhou X (2004) One- and two-photon absorption of three-coordinate compounds with different centers (B, Al, N) and a 2,20-dipyridylnitrogen functional group. J Chem Phys 121:8253–8260

52. Poulsen TD, Ogilby PR, Mikkelsen KV (2001) A quantum mechanical method for calculating nonlinear optical properties of condensed phase molecules coupled to a molecular mechanics fields: a quadratic multiconfigurational self-consistent-field/molecular mechanics response method. J Chem Phys 115:7843–7851

53. Norman P, Luo Y, Ågren H (1999) Large two-photon absorption cross sections in two-dimensional charge-transfer, cumulenecontaining aromatic molecules. J Chem Phys 111:7758–7765

54. Rubio-Pons O, Luo Y, Ågren H (2006) Effects of conjugation length, electron donor and acceptor strengths on two-photon absorption cross sections of asymmetric zinc-porphyrin derivatives. J Chem Phys 124:94310–94314

55. Cronstrand P, Luo Y, Ågren H (2002) Effects of dipole alignment and channel interference on two-photon absorption cross sections of two-dimensional charge-transfer systems. J Chem Phys 117:11102–11106

56. Guo JD, Wang CK, Luo Y, Ågren H (2003) Influence of electron-acceptor strength on the resonant two-photon absorption cross sections of diphenylaminofluorene-based chromophores. Phys Chem Chem Phys 5:3869–3873

57. Wang CK, Zhao K, Su Y, Yan R, Zhao X, Luo Y (2003) Solvent effects on the electronic structure of a newly synthesized two-photon polymerization initiator. J Chem Phys 119:1208–1213

58. Dharmadhikari AK, Sandhu AS, Dharmadhikari JA, Mishra A, Kumar GR (2004) Measurement of two-photon absorption cross-section in organic molecular salt with linear and circular polarized radiation. Appl Phys B 79:235–238

59. Mongin O, Porres L, Charlot M, Katan C, Blanchard-Desce M (2007) Synthesis, fluorescence, and two-photon absorption of a series of elongated rodlike and banana-shaped quadrupolar fluorophores: a comprehensive study of structure-property relationships. Chem Eur J 13:1481–1498

60. Frisch MJ, Trucks GW, Schlegel HB, Scuseria GE, Robb MA, Cheeseman JR, Montgomery Jr JA, Vreven T, Kudin KN, Burant JC, Millam JM, Iyengar SS, Tomasi J, Barone V, Mennucci B, Cossi M, Scalmani G, Rega N, Petersson GA, Nakatsuji H, Hada M, Ehara M, Toyota K, Fukuda R, Hasegawa J, Ishida M, Nakajima T, Honda Y, Kitao O, Nakai H, Klene M, Li X, Knox LE, Hratchian HP, Cross JB, Bakken V, Adamo C, Jaramillo J, Gomperts R, Stratmann RE, Yazyev O, Austin AJ, Cammi R, Pomelli C, Ochterski JW, Ayala PY, Morokuma K, Voth GA, Salvador P, Dannenberg JJ, Zakrzewski VG, Dapprich S, Daniels AD, Strain MC, Farkas O, Malick DK, Rabuck AD, Raghavachari K, Foresman JB, Ortiz JV, Cui Q, Baboul AG, Clifford S, Cioslowski J, Stefanov BB, Liu G, Liashenko A, Piskorz P, Komaromi I, Martin RL, Fox DJ, Keith T, Al-Laham MA, Peng CY, Nanayakkara A, Challacombe M, Gill PMW, Johnson B, Chen W, Wong MW, Gonzalez C, Pople JA (2004) Gaussian 03, Revision C.02. Gaussian Inc., Wallingford

61. Azizi Z, Roos BO, Veryazov V (2006) How accurate is the CASPT2 method? Phys Chem Chem Phys 8:2727–2732

62. Pulay P (2011) A perspective on the CASPT2 method. Int J Quant Chem 111:3273–3279

63. Todorova TK, Gagliardi L, Walensky JR, Miller KA, Evans WJ (2010) DFT and CASPT2 analysis of polymetallic uranium nitride and oxide complexes: hoe theory can help when x-ray analysis is inadequate. J Am Chem Soc 132:12397–12403

64. Leszczynski J (2004) Computational chemistry: Reviews of current trends. World Scientific , Singapore

65. Lahiri A, Ulicny J, Laaksonen A (2004) Theoretical analysis of the excited state properties of wybutine: a natural probe for transfer RNA dynamics. Int J Mol Sci 5:75–83

66. Shukla M, Leszczynski J Jiri S, Filip L (eds) (2006) Comparative study of quantum mechanical methods related to nucleic acid bases: Electronic spectra, excited state structures and interactions. In: Computational studies of RNA and DNA, Springer, New York, pp 433-461